ELECTROMAGNETIC DESIGN OF $\beta = 0.13, f = 325$ MHZ HALF-WAVE RESONATOR FOR FUTURE HIGH POWER, HIGH INTENSITY PROTON DRIVER AT KEK

Gunn Tae Park*, Eiji Kako, Yukinori Kobayashi, Tadashi Koseki, Tomofumi Maruta,
Shinichiro Michizono, Fujio Naito, Hirotaka Nakai, Kensei Umemori, and Seiya Yamaguchi
KEK, High Energy Accelerator Research Organization, Tsukuba, Japan

Abstract

At KEK, a proposal is being prepared for a new linac-based proton driver that can accelerate the proton beam up to 9 GeV with 9 MW beam power and 100 mA peak current. In this report, we present the study on the front end design of the linac, which will accelerate the beam to 1.2 GeV: The baseline layout, the acceleration energy structure, RF characteristics of components, cryomodule configurations, and the detailed design of half-wave resonator 1.

INTRODUCTION

A new multi-MW proton driver with 100 mA peak current is being planned for neutrino physics at KEK [1]. A proposed set of beam parameters for neutrino physics is listed in Table 1.

Table 1: Beam Parameters

Beam parameters	Unit	Value
Energy	GeV	9
(Peak) current	mA	100
Power	MW	9
Pulse length	ms	1
Repetition rate	Hz	10

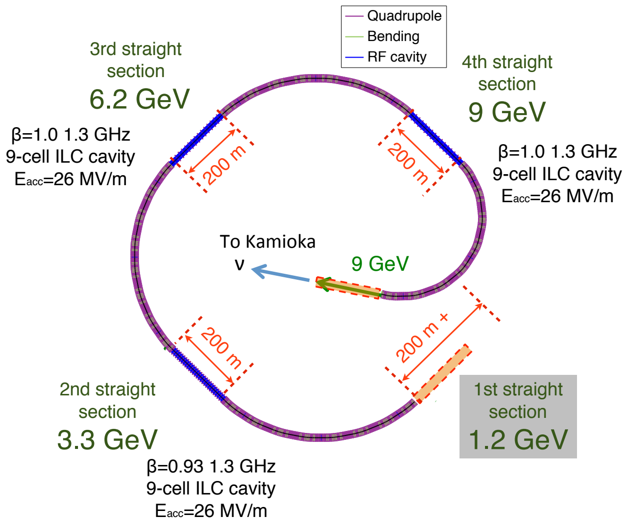

Figure 1: The tunnel configuration of the proton driver

The driver is being considered to be located at KEKB tunnel, whose view is shown in Fig. 1. The driver will use four 200 m long straight sections of the tunnel for a linac. While the rest of straight section will be accelerated with $\beta \sim 1$ by TESLA-type 9-cell elliptical cavities, the front end of the linac that uses the 1st straight section is expected to accelerate the proton beam up to 1.2 GeV using superconducting low-beta cavities.

This report is summary of the studies done to design the front end of the linac: baseline layout, choice of accelerators and their specifications, and the design of the first accelerator in the beamline, the superconducting half-wave resonator 1 (HWR1).

BASELINE LAYOUT

The front end of the linac consists of electron cyclotron resonator (ECR) ion source, low energy beam transport (LEBT), radiofrequency quadrupole (RFQ), medium energy beam transport (MEBT), 3 types of low-beta superconducting cavities (half-wave resonator 1, half-wave resonator 2, single spoke resonator), and 2 types of 5-cell elliptical cavities (medium beta elliptical cavity (MBE) and high beta elliptical cavity (HBE)) as shown in Fig. 2.

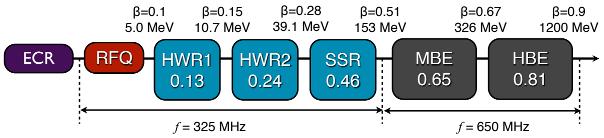

Figure 2: Layout of the front-end baseline. The blue and the grey are low energy and high energy linac, respectively.

The base frequency is determined by that of the RFQ, which is set at 325 MHz. The detailed specifications of the components of the front end is listed in Table 2.

HALF-WAVE RESONATOR 1

The half-wave resonator 1 is optimized for $\beta = 0.13$ with frequency $f = 325$ MHz. High intensity beam current requires a large bore radius of $R_{bore} = 20$ mm. Because relatively large frequency bandwidth is expected with a high beam loading, the helium pressure fluctuation is not expected to impact the tuning and the operating temperature is set to be 4.2 K.

---

[*] gunnpark@post.kek.jp

Copyright © 2016 CC-BY-3.0 and by the respective authors

Table 2: RF Parameters of Linac Components

Parameters	HWR1	HWR2	SSR	MBE	HBE
f (MHz)	325	325	325	650	650
n_{cell}	2	2	2	5	5
β_{opt}	0.13	0.24	0.46	0.61	0.76
β_{in}	0.1	0.15	0.28	0.51	0.67
β_{out}	0.15	0.28	0.51	0.67	0.9
V_{acc} (MV)	0.7	2.1	5.3	10.2	15.4
ϕ_s (rad)	−30	−30	−27	−27	−27
G (Ω)	40	73	117	192	236
E_p/E_{acc}	6.9	4.8	4.1	2.5	2.4
B_p/E_{acc}	14.2	6.2	7.9	4.6	4.4
P$_{beam}$ (kW)	53	182	473	909	1373
n_{cav}	10	20	30	20	72
n_{cav}/cm	5	4	5	4	3

The unit for B_p/E_{acc} is mT/(MV/m).

Electromagnetic Design

Electromagnetic design of the cavity was optimized for figures of merit including high cavity voltage V_0, low peak magnetic field B_p, and high geometrical factor G. The thresholds for the peak electric and magnetic fields are set to be $E_p = 35$ MV/m and $B_p = 120$ mT respectively. The structure of the resonator was modified from the simple co-axial geometry. The re-entrant nose was introduced to keep the gap g and center of the gap-to center of the gap distance d while increasing the outer radius of cavity. The drift tube was shaped into the ring for minimal axial asymmetry of the accelerating field. This is important specially with our plan to use superconducting solenoid as a focusing element, which has only axis-symmetric component. Finally, the center conductor was tapered to reduce the peak magnetic field.

The dimensional parameters of the cavity were optimized by using 3D FEA code CST-MWS, following the standard procedure [2], [3]. The optimized HWR1 is shown in Fig. 3.

Table 3: RF Figures of Merit of the HWR1

Figures of merit	**Value**	**Figures of merit**	**Value**
f [MHz]	325	E_p [MV/m]	35
β_{op}	0.13	B_p [mT]	72
V_0 [MV]	0.78	E_p/E_{acc}	6.9
E_{acc} [MV/m]	5.1	B_p/E_{acc}	14.1
$\mathcal{R}/Q_0$	384	P_0 [W]	0.4
TTF	0.78	G [Ω]	40.2
T [K]	4.2	Q_0	3.3×10^9

The unit for B_p/E_{acc} is [mT/(mV/m)].

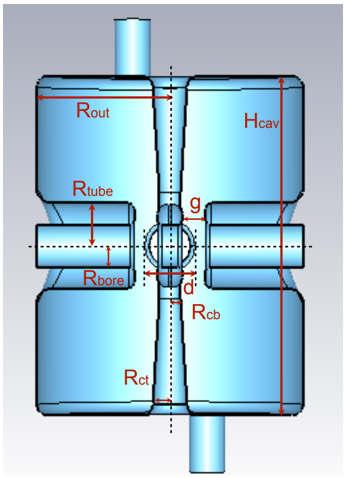

Figure 3: The sectional view of the HWR1.

The corresponding figures of merit are listed in Table 3. In the Table, E_{acc} is obtained from dividing V_{acc} by the effective length $L_{eff} = \beta_{op}\lambda$. In Fig. 4, the electromagnetic field distribution is shown. The electric field is dominant near beam axis (See Fig 4(a)), while the magnetic fields are uniformly distributed over the center conductor (See Fig. 4(b)). In Fig. 5, the transverse field asymmetry, defined as $E_y(y = 3.5mm) - E_z(z = 3.5mm)$ with the expected *rms* beam size being 3.5 mm, is plotted. The maximum asymmetry is only 4×10^4 V/m, less than 1% of the accelerating field gradient. With most of power accounted by beam power in heavy beam loading, the generator power available at cavity is about 52 KW and the loaded quality factor $Q_L \sim 3 \times 10^4$, leading to the bandwidth of 10 kHz.

Multipaction

The multipaction was studied with the simulation by using CST-PS. In the simulation, we used SEY (secondary electron yield) of the niobium with wet treatment as shown in Fig. 6. The experimental measurement of SEY of the niobium with the standard surface treatment at KEK at $K_e = 1$ keV with DC current [4] indicates that $\langle\delta\rangle \sim 1.7$ and closely resembles the one with wet treatment. Two major multipactions are predicted. One is at low accelerating gradient, taking place inside the drift tube. (See Fig. 8) The other is near operating accelerating gradient, taking place at the top and bottom toroids. The trajectories of the electrons are cyclotronic with centrifugal force fed by magnetic field, leading to 2-point multipaction. The voltage bandwidth for the multipaction is wide spread as shown in Fig. This is familiar multipaction to the HWR, as reported in [5]. The effort to avoid the multipaction is underway.

CONCLUSION

The front end design of the linac for the multi MW proton driver at KEK is done determining on acceleration sections, superconducting cavities, and their specifications. The opti-

Copyright © 2016 CC-BY-3.0 and by the respective authors

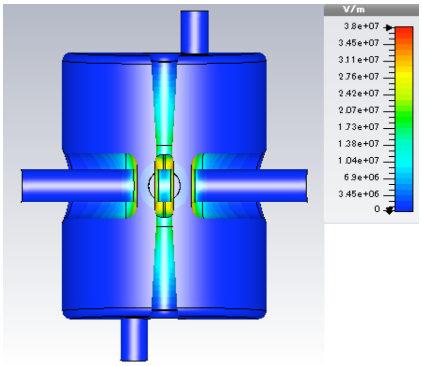

(a) The electric field

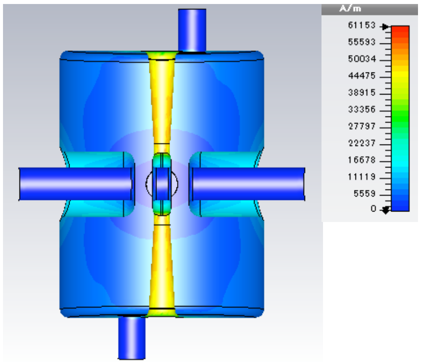

(b) The magnetic field

Figure 4: The electromagnetic field distribution of the HWR.

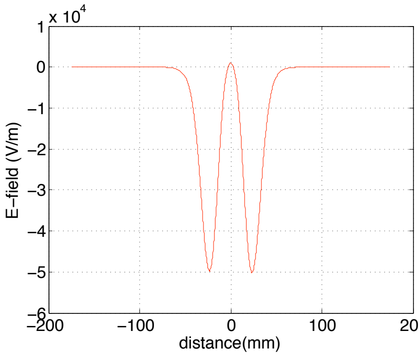

Figure 5: The transverse field asymmetry.

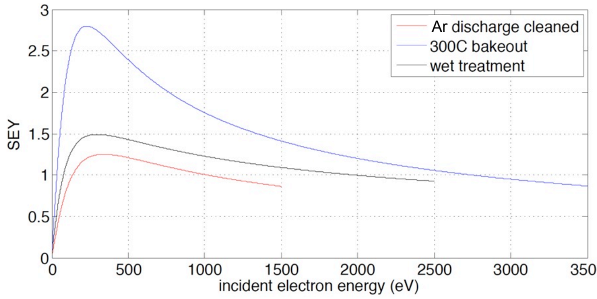

Figure 6: The SEY curves of niobium with various surface treatments.

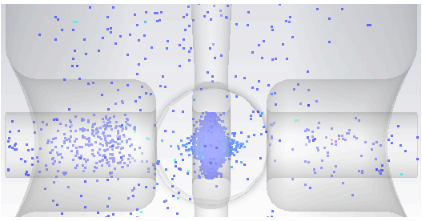

(a) The trajectory of electrons during multipaction

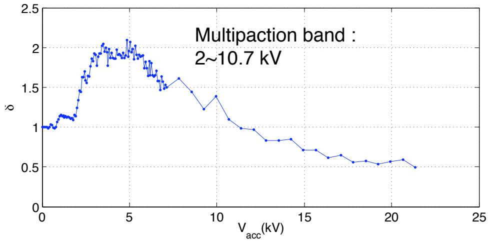

(b) Multipaction voltage band

Figure 7: The multipaction of the HWR1 near beam port.

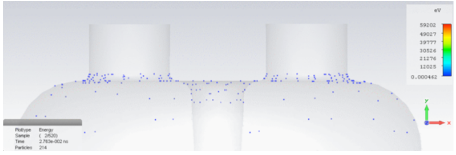

(a) The trajectory of electrons during multipaction

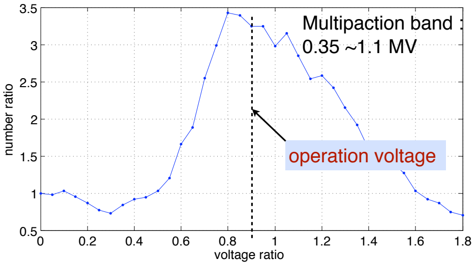

(b) Multipaction voltage band

Figure 8: The multipaction of the HWR1 near beam port. In (b), number ratio is number of electrons after 12.3 ns to that after 3.1 ns. Voltage ratio is voltage to V_{acc}. Operational voltage includes the synchronous phase term.

mized electromagnetic design and multipaction study of the $\beta = 0.13$, $f = 325$ MHz half-wave resonator is presented.

REFERENCES

[1] T. Maruta *et al.*, "Design study on the 9 GeV proton linac at KEKB tunnel for the next generation neutrino experiment", JPS Conf. Proc. vol. 8, p. 011013, 2015.

[2] B. Mustapha *et al.*, "Electro-magnetic optimization of a half-wave resonator", in *Proc. of SRF'11*, Chicago, IL, USA, paper MOPO044.

[3] S. Miller *et al.*, "Design for manufacture of superconducting half wave cavities", in *Proc. of SRF'11*, Chicago, IL, USA, paper MOPO051.

Copyright © 2016 CC-BY-3.0 and by the respective authors

[4] R. Noer *et al.*, “Secondary electron yield of Nb RF cavity surfaces", Proceedings of the 10th Workshop on RF superconductivity2001, Tsukuba, Japan.

[5] Z. Zheng *et al.*, “Multipacting simulation and analysis for the FRIB superconducting resonators using TRACK3P”, THP092, Proceedings of LINAC2010, Tsukuba, Japan.

ISBN 978-3-95450-147-2

Copyright © 2016 CC-BY-3.0 and by the respective authors